

7

Permissible Aquifer Recharge Rates and its Sensitivity towards aquifer and well parameters

7.1 INTRODUCTION

The site characteristic is of paramount importance in determining the maximum baseflow that can be restored through the application of an ASR system. It has been established from the previous chapter that the flux restored in the river is directly proportional to the quantity of the injected water. Kumar et al. (2024) have defined the optimal injection rate under the given operational and geological constraints as the permissible aquifer recharge capacity (PARC) of an ASR site. They have utilized a linear regression model to determine PARC by mapping the relation between injection rate and head buildup at the grid cells of a numerical model. The method presented is fast and computationally efficient at the expense of the uncertainty raised due to the simplification of the MODFLOW model outputs to a linear response function. Improving on the concept presented by Kumar et al. (2024), we modify the metric name PARC as Permissible Aquifer Recharge Rate (PARR), which is more suitable for allowable recharge rate (Kumar et al., 2025).

In this study, a novel optimization approach has been presented to determine PARR with numerical GW flow models to reduce this uncertainty and computational time. The methodology utilizes the analytical relationship between injection rate and corresponding head buildup for confined and unconfined aquifers given by Theis (1935) and Neuman (1972).

The aquifer recharge capacity is highly dependent on the hydrogeological (Transmissivity, Aquifer thickness, Storativity, and aquifer type) and well characteristics (skin layer hydraulic conductivity, well radius, and well losses) (Hugman et al., 2012; Shandilya et al., 2022a; Tiwari and Yadav, 2024). The effect of well operation parameters (skin factor, wellbore storage, and pumping duration) on pumping capacity has been thoroughly analyzed by Shandilya et al. (2022a) with the analytical solution given by Agarwal et al. (1970). The recovery efficiency of an ASR project is highly correlated with the aquifer's transmissivity and thickness (Tiwari and Yadav, 2024). A sensitivity analysis of model parameters is crucial for assessing the significance of model parameters and their uncertainty (Baker et al., 2023, 2022). Sensitivity analysis offers insights into how changes in management practices may affect GW resources, enabling informed decision-making (Bianchi Janetti et al., 2019; Reinecke et al., 2019). Based on the current literature, assessing the sensitivity of various decision-making parameters (aquifer and operational) on PARR is essential for its wide application. Local sensitivity analysis deals with the sensitivity of model outputs to small variations in individual input parameters. In contrast, global sensitivity analysis examines the sensitivity of model outputs to the entire range of possible input parameter values (Tang et al., 2007). Since previous literature does not include global sensitivity (Shandilya et al., 2022a), combined local and global sensitivity analyses were performed here to assess the important factors affecting PARR.

One powerful global sensitivity analysis method is Sobol's sensitivity indices, which quantify the contribution of individual input parameters and their interactions to the total variance of the model output (Song et al., 2015). This approach has been widely applied in various fields, including hydrology, environmental modeling, and economic evaluation of healthcare technologies (Bianchi Janetti et al., 2019; Briggs et al., 1994; Gan et al.,

2014). Reinecke et al. (2019) found the sensitivity of aquifer and hydrological parameters to the global simulated head of the global gradient-based GW model. Tang et al. (2007) compared the performance of Sobol's sensitivity analysis with other popular methods, such as local analysis, regional sensitivity analysis, and analysis of variance, in the context of a rainfall-runoff model and found that Sobol's method yielded more robust sensitivity rankings. The sensitivity of the parameters affecting the PARR is a critical consideration for designing and implementing ASR projects at a site.

This chapter discusses the detailed conceptualization of PARR and a more accurate method to determine it from numerical models. The factors influencing PARR have been analyzed, and their local and global sensitivity has been assessed with Sobol's indices.

The main objectives covered in this chapter are as follows:

- Determination of PARR through an adaptive learning-based optimization approach.
- Analysis of the global and local sensitivity of PARR.

7.2 PERMISSIBLE AQUIFER RECHARGE RATE (PARR)

7.2.1 Analytical Definition

Shandilya et al. (2022a) defined the storage capacity of an aquifer for a given set of operational parameters (duration and well characteristic) as the maximum volume of water that can be injected or extracted under the limit of permissible head change. The duration of pumping has been stated as an important factor along with the wellbore storage and skin factor (Martinez and Widdowson, 2023; Shandilya et al., 2022a). Without time constraints, any large volume of water can be stored, even in subpar aquifers, demonstrating the importance of pumping duration in injection well design. The duration constraint is also essential due to the temporal availability of water for the ASR.

The permissible aquifer recharge capacity (PARR) has been defined as the maximum injection rate to an aquifer for a given operational time (and well characteristics) under the constraints of a permissible head (*such that* $\text{PARR} \times \text{Injection duration} = \text{Aquifer storage capacity}$) (Kumar et al., 2024). The permissible head is required to avoid waterlogging or flooding in unconfined aquifers or to prevent the confining layer’s failure in confined aquifers (Shandilya et al., 2022b). As the water is injected into the aquifer with a constant recharge rate, the head rises near the screen and propagates towards the confining layer or water table (Welch et al., 2013). The pressure head developed near the confining layer at the critical location (mainly near the injection well) can rupture the confinement of confined aquifers or raise the water table to cause flooding in unconfined aquifers. The optimal injection rate for a given duration, which does not cause flooding in water table aquifers and failure of the confining layer in the confined aquifer, is called PARR. **Figure 7.1** illustrates the head developed due to injection with respect to time. The value of PARR has been demonstrated in both analytical solutions (**Figure 7.1A**) and real-world scenarios (**Figure 7.1B**). The value of PARR is associated with the optimal pumping rate (Q), which generates a head equal to H_{per} in the injection duration of t_{end} .

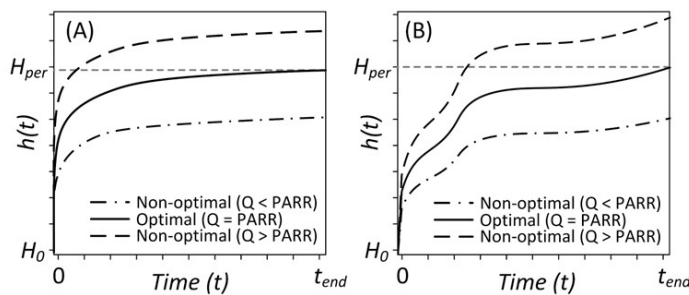


Figure 7.1. The definition of PARR as per (A) the analytical solutions (modified from Sandilya et al. 2022) and (B) the real field scenario.

The relationship between the recharge rate and the corresponding head development is crucial for the determination of PARR (Kumar et al., 2024). The analytical solutions for

the 2D GW flow for pumping/injection wells have been developed by several authors, starting from (Theis, 1935), where he assumed the aquifer to be homogeneous and isotropic to an infinite extent. The assumption regarding the well losses (i.e. Skin layer effect (Van Everdingen, 1953), wellbore storage (Agarwal et al., 1970), partial well-penetration (Hantush, 1964), unconfined conditions (Neuman, 1972) and inter-aquifer leakages) have been further taken into consideration to refine the Theis' solution. Considering no losses in the well, the head developed in the well is equal to the head near the well casing for a fully penetrated case and generally given as.

$$h = h_0 + \frac{Q}{4\pi T} W(u) \quad 7.1$$

Where h_0 and h are the initial head and head at time t , respectively. Q is the pumping/injection rate, and T is the transmissivity of the aquifer. The $W(u)$ is the function of one or several parameters depending on the well characteristics and aquifer type, generically known as the well function. The well functions for confined and unconfined aquifers have been presented in **Table 7.1**. If $W(u)$ does not depend on the Q (i.e. neglecting the nonlinear head loss) for a given pumping duration, the value of $W(u)$ is constant at a fixed radial distance (r) from the well. Therefore, the optimal water injection rate ($PARR$) is determined such that the injected volume is maximized while ensuring that the head near the well ($r = r_w$) at the end of injection ($t = t_{end}$) equals the permissible head (H_{per}).

$$PARR = \frac{4\pi T \cdot (H_{per} - h_0)}{W|_{r=r_w, t=t_{end}}} \quad 7.2$$

7.2.2 Numerical Solution

Since the analytical 2D solution to the well does not consider the effect of nearby sources and sinks (Freeze and Cherry, 1979), it is imperative to utilize 3D numerical models to determine the aquifer scale recharge capacity, especially for a complex GW system. Numerical GW models (such as MODFLOW) have been utilized in many projects worldwide due to their versatility and accuracy in complex studies (Freeze and Witherspoon, 1966; Kuiper, 1983), following advancements in computing power. Due to the forward modelling approach of MODFLOW, the direct determination of PARR is impossible and hence requires an iterative method to find the optimum solution. The forward simulation determines the heads with given stresses and boundary conditions in a numerical model. A simple optimization approach is generally needed to determine the PARR by maximizing the net injected water volume for a given injection duration.

$$\text{maximise}(Q_i \times t_{end})$$

$$\text{Such that } (h_{i,t}|_{Q=Q_i,t=t_{end}} - H_{per}) \leq \epsilon \quad 7.3$$

Where Q_i represents the injection rate [L^3T^{-1}] at location i , $h_{i,t}$ is the simulated head [L] with Q_i at the end of the injection duration (t_{end})[T], and ϵ is the tolerance limit [L] which is the acceptable difference between actual permissible head and simulated head at the end of injection.

Since the head varies monotonically with time, the optimization method eventually converges to the maximum recharge rate, creating a head equal to H_{per} at $t = t_{end}$. The optimization method can be time-consuming with a numerical model, especially with real-field complex models. The number of iterations required to find the optimum solution in GW problems often depends on the choice of the learning rate. Selecting an optimal

learning rate is crucial; a rate too low may result in slow convergence, whereas a rate too high could lead to oscillation around the minimum or divergence of the loss function (Ruder, 2017). The dynamic learning rate based on known properties of the objective function, such as the relation between recharge rate and corresponding head change, can help address this issue (Tholeti and Kalyani, 2020) we devised an adaptive learning rate method that computes PARR using linear relation of injection rate and head developed, requiring minimal additional computation compared to gradient descent (Zeiler, 2012). Given that $t = t_{end}$, the equation (7.1) can be rewritten as:

$$h_{i,t} = h_0 - \frac{Q_i}{4\pi T} \cdot W|_{r=r_w, t=t_{end}} \quad 7.4$$

Here, at a particular time (t_{end}) and at a fixed distance from the well (in this case equal to the radius of the well (r_w)), the value of the well function becomes constant, and the **Eq. 7.4** becomes linear (**Figure 7.2**).

$$Q_i = C_1 - C_2 h_{i,t} \quad \text{where } C_1 \text{ and } C_2 \text{ are constants} \quad 7.5$$

After simulating the model with a selected upper and lower bound of Q_i , we utilized the linear relationship to determine the first estimate PARR. The constraint of the maximum head simulated at the end of the injection is checked with the permissible head. The estimated PARR is accepted if the residual is within the tolerance limit. The tolerance limit controls the number of iterations required to determine PARR. A lower value will yield more accurate estimation while requiring more iterations. During the implementation of the proposed methodology, it has been observed that in the case of a confined aquifer, it took only 5-12 iterations to determine PARR with a tolerance of 1

mm. However, In the case of an unconfined aquifer, the number of iterations required was in the range of 8-56 for a tolerance of 1 mm.

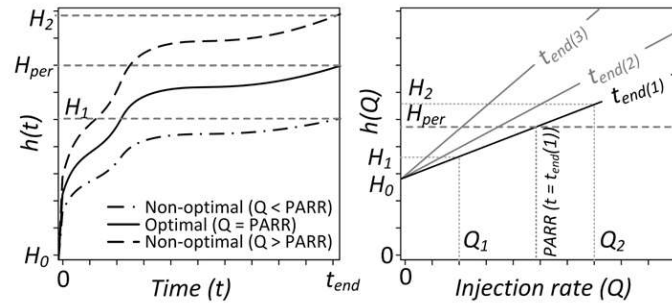


Figure 7.2. The determination of PARR with simulated heads (The linearity between h and Q for a given injection duration is shown in the figure on the left. The slope of the h vs Q curve depends on the injection duration.)

In the case of unconfined aquifers, the relation between Q and h is nonlinear (Martinez and Widdowson, 2023), i.e. the calculated maximum head corresponding to the initial estimate of PARR can be lower or higher than the permissible head. The upper or lower bound is updated with the estimated Q , depending upon the residual characteristic. The linear relationship is fitted again to find the next Q value corresponding to H_{per} . Since the relation between the head and the injection rate is monotonously increasing, the dynamic learning rate helps in the estimation of the optimal value of PARR under the tolerance limit faster. The method has been presented in **Figure 7.3**.

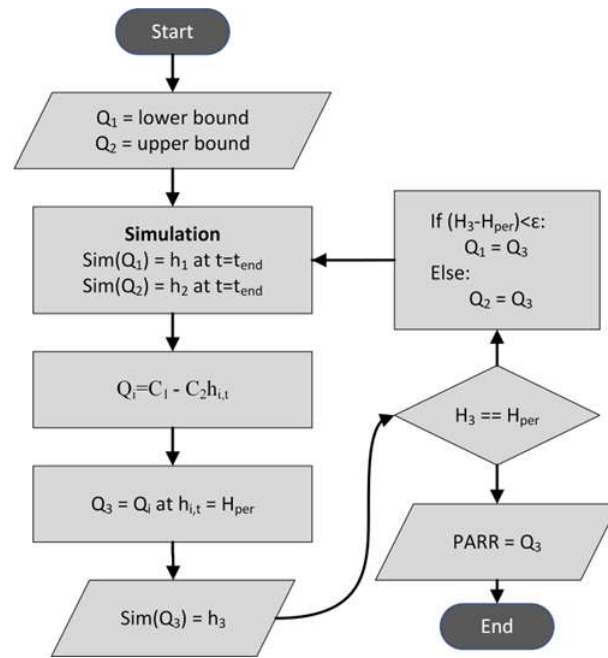


Figure 7.3. Flow chart for the calculation of PARR with MODFLOW simulation.

7.3 THE PERMISSIBLE AND RECOVERABLE HEAD

The head generated in the aquifer in response to the injection rate can result in undesirable effects (fracture of confining layer, flooding, or generation of artesian conditions) (Shandilya et al., 2022b). The increased hydraulic head near the injection well in the confined aquifer can damage the confining layer if increased beyond the safety limit of overburden pressure (Parker et al., 2022b). The permissible head (H_{per}) refers to the maximum allowable pressure head that can be achieved at the injection site without inducing any adverse effects. The difference between the initial and permissible head is termed the recoverable head ($H_{per} - h_0$) and is an essential criterion in determining PARR. The larger recoverable head represents the more significant GW deficiency, resulting in a higher value of PARR and vice versa.

In the case of a confined aquifer, the permissible head is calculated by estimating the overburden pressure at the critical location of the confining layer near the well. For a

geological layered system with minor principal stress oriented in the horizontal direction, the permissible head for a confined aquifer is given as (Shandilya et al., 2022b).

$$H_{per} = h_o + h_{fp}(1 - SF) \quad 7.6$$

$$h_{fp} = \sum_{i=1}^n \left(\left(\frac{\mu_i}{1 - \mu_i} \right) \left(\frac{\rho_{oi}}{\rho_w} D_i - h_{pi} \right) + h_{pi} \right) + \left(\frac{P_o}{\rho_w g} \right) \quad 7.7$$

Where, H_{per} is the permissible head [L], h_o is the initial head [L], h_{fp} represents the fracture pressure head of the confining layer [L], SF is the factor of safety, μ_i is the Poisson's ratio of overburden soil, ρ_{oi} is the density of overburden soil [ML-3], ρ_w is the density of water [ML-3], D_i is the thickness of the confining layer [L], h_p is the pore water pressure head [L], P_o is the atmospheric pressure [ML-1T-2], and g is the acceleration due to gravity [LT-2].

In the case of an unconfined aquifer, the allowable head is constrained by the chance of flooding or generation of artesian conditions in the vicinity of the injection well. The permissible head is selected based on site-specific conditions, such as avoiding the rootzone depth in the agricultural area or the foundation depth of the building in a residential area and government norms (Shandilya et al., 2022b).

7.4 SENSITIVITY ANALYSIS

A hypothetical homogeneous numerical model for confined and unconfined aquifers has been developed with the representative data presented in **Table 7.1** to demonstrate the proposed methodology for the determination of PARR and the sensitivity analysis (local

and global). The models have been discretized into ten layers and a varying cell size from 10m at the injection well (in the center) to 1000m at the boundaries. The model dimension has been established so that the influence area of the well never reaches the boundary to avoid sudden head change. The left and right boundaries have been taken as Dirichlet's boundary (specified head), such that a head loss of 5 meters occurs from left to right in both cases (i.e. confined and unconfined). This sets a starting steady state head of 57.5m at the well location for the confined aquifer and 52.56m for the unconfined aquifer. The other two boundaries have been taken as no-flow boundaries. Before performing the transient simulation, the steady-state starting head has been established before applying the injection well by running the model in steady-state simulation. The injection well has been modeled with the MNW2 package (Leonard F.Konikow, George Z. Hornberger, Keith J. Halford, 2009) to accurately control the screen placement and size.

Table 7.1. Hypothetical model conceptualization

Aquifer Type	Properties	Base Values	Range
Confined	Dimension	10km * 10Km * 50m	-
	Hydraulic conductivity (H_k)	0.001 (m/sec)	$1.15 \times 10^{-04} - 0.05$ (m/sec)
	Specific storage (S_s)	1.0×10^{-04}	$1.0 \times 10^{-07} - 0.001$
	Horizontal anisotropy ($HANI$)	1.0	0.25 - 10
	Vertical anisotropy ($VANI$)	3.0	1 - 10
	Well screen length (L_{sc})	50m (<i>fully penetrated</i>)	2 – 30 (m)
	Well Screen Location (Center) (H_{sc})	25m	15 – 35 (m)
Un-confined	Dimension	10km * 10Km * 60m	
	Hydraulic conductivity (H_k)	0.001 (m/sec)	$1.15 \times 10^{-04} - 0.05$ (m/sec)

Specific yield (S_y)	0.2	0.01 – 0.4
Horizontal anisotropy ($HANI$)	1.0	0.25 - 10
Vertical anisotropy ($VANI$)	3.0	1 - 10
Well screen length (L_{sc})	50m (<i>fully penetrated</i>)	2 – 30 (m)
Well Screen Location (Center) (H_{sc})	25m	15 – 35 (m)

7.4.1 Local Sensitivity of PARR

7.4.1.1 Effect of Aquifer Parameters on PARR

The characteristics of the aquifer, such as hydraulic conductivity and storage coefficient, play a vital role in determining the maximum injection rate under the allowable constraints (Shandilya et al., 2022a). The effect of aquifer hydraulic conductivity (H_k), specific storage (S_s), horizontal anisotropy ($HANI$), and vertical anisotropy ($VANI$) has been analyzed and presented for four injection durations (1 hr, 1 day, 1 month, and 1 year). The representative value range of aquifer parameters has been taken to analyze the PARR's local sensitivity and tabulated in **Table 7.1**. The value range has been chosen to represent the general characteristics of the aquifer and the constraints of screen length (L_{sc}) and location (H_{sc}) based on aquifer dimensions. The L_{sc} is set at 50m for confined and unconfined conditions, representing a fully penetrated well in the base scenario. Given the assumed 50m thickness of the aquifer, L_{sc} cannot exceed this. By varying L_{sc} between 2-30m, we create adequate space and enable H_{sc} to vary between 15m – 35m, remaining within the aquifer thickness.

The PARR has shown a nonlinear relation with the aquifer parameters, and the slope of the curve depends on the duration of injection. The variation of PARR with respect to aquifer and well parameters has been plotted in **Figure 7.4** and **Figure 7.5**. It should be noted that although the fitted curve appears linear for a large injection duration, it is

actually non-linear. The fitted curve, along with its correlation coefficients, is provided in **Table G.1** in the appendix.

In the case of the confined aquifer, the PARR is non-linearly correlated to the H_k (fitted to the polynomial function of 2nd order) and shows high sensitivity (**Figure 7.4(1.A)**). As H_k increases, the head developed for the given injection rate decreases, resulting in a high injection rate to reach the H_{per} . For a longer duration, the fitted curve between H_k and PARR tends to become linear. The PARR increases with S_s with a large gradient for $S_s < 0.00012$ and further with a lower gradient after $S_s \approx 0.00012$ (**Figure 7.4(1.B)**). The PARR is insensitive to $VANI$ as it shows insignificant variation with $VANI$ (**Figure 7.4(1.C)**). The PARR for the fully penetrated well in the confined aquifer is insensitive to vertical anisotropy. It is justified by the assumption of radial flow in a fully penetrated confined aquifer (Theis, 1935). The increased horizontal anisotropy results in high conductivity in one of the horizontal principal planes, necessitating a high injection rate to achieve head rise and vice versa. This results in a higher value of PARR (**Figure 5(1.D)**); hence, PARR shows considerable sensitivity to $HANI$.

The PARR also varies non-linearly with H_k for the unconfined aquifer (**Figure 7.4(2.A)**) and has been fitted with the polynomial function of 2nd order. The PARR also shows polynomial variation with S_y and has a higher gradient for the smaller duration of Injection (**Figure 7.4(2.B)**). The gradient attenuates for a higher injection duration. The PARR is sensitive w.r.t the vertical anisotropy ($VANI$) in the case of an unconfined aquifer and can be fitted by 2nd order polynomial function (**Figure 7.4(2. C)**). The sensitivity of PARR to $HANI$ again follows the polynomial function with a high gradient (**Figure 7.4(2.D)**).

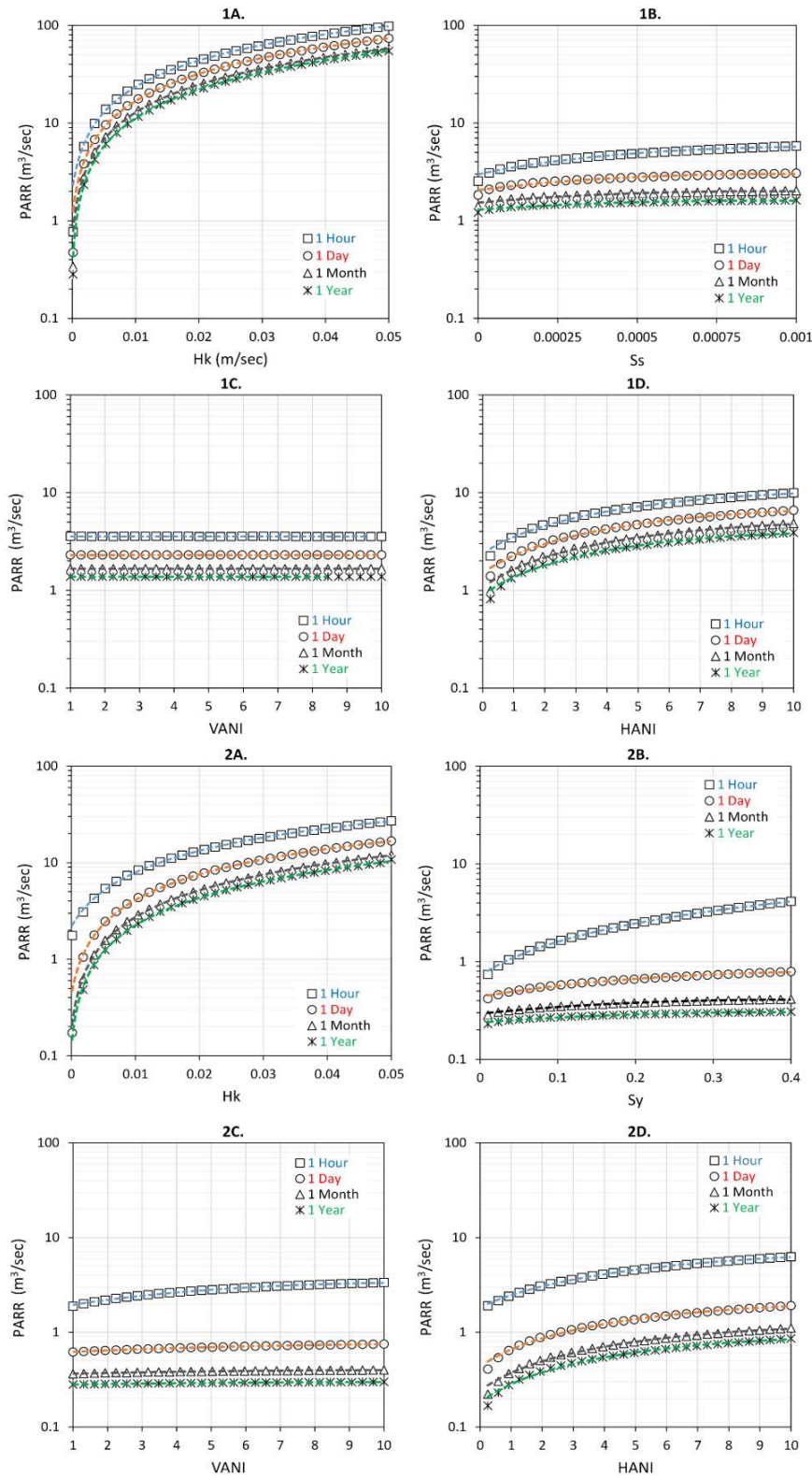


Figure 7.4. The local sensitivity of PARR with aquifer parameters in the (1) confined aquifer and (2) unconfined aquifer (A. linear plot between PARR and Hk; B. linear plot w.r.t Ss or Sy; C. linear plot w.r.t VANI and D. linear plot w.r.t HANI)

7.4.1.2 Effect of location and length of well screen on PARR

The analytical solution for the head dissipation by Jenkins et al. (2019) suggests that the dissipation of the head raised due to water injection into the aquifer depends on the time and aquifer conductivity. The time required for the head to propagate to the top of the aquifer is inversely related to the aquifer conductivity (Welch et al., 2013). It makes the starting location of head propagation or the location of initial fluid potential (Freeze and Cherry, 1979) important for determining PARR since the time required for the head to propagate to the critical point in the case of a confined aquifer and the water table in the case of an unconfined aquifer depends on the starting location. This elapsed time contributes to the delayed response of injection to the head at the critical point (Neuman, 1972), leading to high PARR values for shorter injection durations.

As per the previous discussion, the location of the well screen plays a significant role in determining PARR, as the induced water pressure propagates from the screen location to the aquifer. The phenomenon is more prominent in the case of aquifers with significant thickness, where a fully penetrated well is not feasible. The partial penetrating well leads to a vertical component of GW flow near the well in the case of the confined aquifer, which was insensitive to the vertical anisotropy in the case of a fully penetrated well. It raises a decision-making problem for the well-screen location in the aquifer.

The sensitivity of PARR w.r.t the location of the screen (H_{sc}) and the screen size (L_{sc}) provides insights for determining suitable screen size and location within the aquifer. The PARR has been determined by varying the screen size. Additionally, the effect of screen location on PARR has been analyzed by changing the screen's centroid location (H_{sc})

while keeping the screen size (L_{sc}) fixed at 3 meters. The combined effect of L_{sc} and H_{sc} on PARR has also been presented in **Figure 7.5(1C & 2C)**.

The PARR value decreases with increasing H_{sc} for confined and unconfined aquifers for all periods. The 3rd-order polynomial equations and R^2 values indicate an excellent fit in **Figure 7.5(1A & 2A)**. The trends show that the PARR decreases as the screen elevation increases, with the most significant change occurring within the first hour (*i.e. small duration*) and the least significant over a year (*i.e. long duration*). Like H_{sc} , the PARR value increases with increasing L_{sc} for all periods. The 3rd-order polynomial function well explains the variation. Similar to H_{sc} , the trends show that as the L_{sc} increases, the PARR increases, with the most significant change occurring within the first hour and the least significant over a year **Figure 7.5(1B & 2B)**. The variation of PARR with L_{sc} also depends upon the location of the screen. As the screen is placed on the top aquifer, where the critical location exists, the PARR increases as the L_{sc} increases. However, if placed at the bottom of the aquifer, the value of PARR decreases as L_{sc} increases. The phenomena can be justified by the propagation of the pressure head, with the placement of the screen near the critical point. As the screen size increases towards the critical point, the time for head propagation decreases, and the permissible head reaches earlier, resulting in lower PARR values.

In the case of an unconfined aquifer, the water table buildup occurs due to mass balance rather than a change in pressure. The injected water creates the head mound, which is continuously propagated in the radially outward direction, resulting in a continuous increase of influence area (Chahar, 2015). Neuman (1972) derived an analytical solution to map the delayed response of the unconfined aquifer to pumping/injection. The water table rises at a lower rate in the unconfined aquifers when compared to Theis' solution (Confined aquifer) (Freeze and Cherry, 1979). When the screen size varies from the

bottom, large values of PARR are observed, which decrease as the top of the screen approaches the saturated thickness.

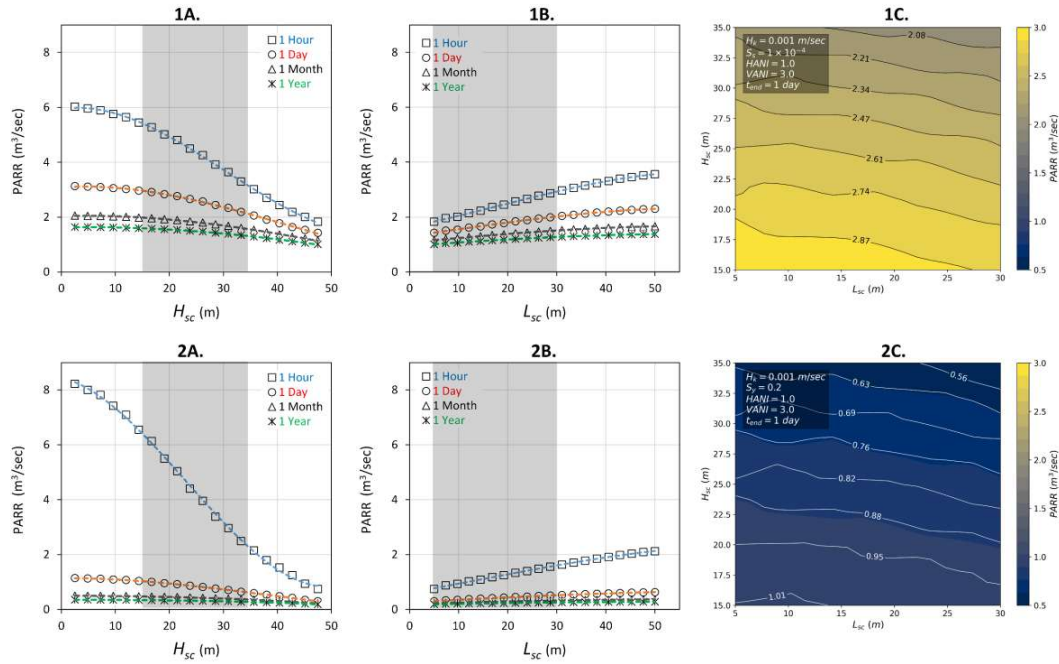


Figure 7.5. The variation of PARR w.r.t well characteristic in (1) confined aquifer and (2) Unconfined aquifer (A. w.r.t screen location (H_{sc}) (the location of the centroid of the screen is varied from bottom to the saturated thickness of the aquifer) B. w.r.t screen size (L_{sc}) and C. contour plot depicting the combined effect of screen size and location.)

In **Figure 7.5**, plots 1C and 2C provide a detailed visualization of how the parameters H_{sc} and L_{sc} jointly influence the PARR values. In both contour plots, it is evident that PARR values are highest when H_{sc} is at its minimum and L_{sc} is at its maximum. This trend illustrates a clear inverse relationship between H_{sc} and PARR and a direct relationship between L_{sc} and PARR. As H_{sc} increases, PARR values decrease, showing a strong gradient, especially in the mid-range of the contour plot. Conversely, as L_{sc} increases, PARR values rise, indicating the significant impact of the screen length on the output. The contour lines in both graphs are closely spaced, signifying step changes in PARR values with slight variations in H_{sc} and L_{sc} . It was found that the head attenuation caused by screen location was higher than by screen size when determining PARR. Since PARR

is more sensitive to the screen location than size, the screen should be placed near the bottom of the aquifer in case of partial penetrating well. The screen size is a design problem of the well and requires an assessment of head losses caused by higher exit velocity. This has been discussed by Pyne (2017) and van Lopik et al. (2021) in detail.

7.4.2 Global Sensitivity Analysis

Sensitivity analysis is an important part of scientific research and modelling because it helps researchers understand the relative relevance of numerous input variables in affecting the output of a complex system. Sobol's method (Sobol, 1993) is a global sensitivity analysis technique that quantifies each input variable's contribution to output variation while accounting for all interactions. It performs particularly well in complex, nonlinear models. The method uses variance decomposition to generate sensitivity indices, also known as Sobol's indices, for each input parameter.

The original Sobol's method, used for sensitivity analysis, required $n \times (2m+1)$ model runs to estimate sensitivity indices, where n is the sample size, and m is the number of parameters. To improve this method, (Saltelli, 2002) developed an enhanced version that can compute the first, second, and total order sensitivity indices using $n \times (2m+2)$ model runs. This enhancement allows for a more comprehensive analysis of the contribution of each parameter to the overall variance.

The aquifer's response to injection is complex, depending upon multiple aquifer and operational parameters. The conventional approach of local sensitivity analysis (Shandilya et al., 2022a; Wang and Luo, 2021), which evaluates the impact of individual parameters, may not be sufficient to capture the combined effects of multiple parameters on the system response. Performing global sensitivity analysis can help identify the most

influential parameters that control the model outputs. Sobol's method is a widely used global sensitivity analysis technique that can decompose the variance in model outputs into the contributions from individual parameters and their interactions (Andrews, 2008). It has been widely applied to environmental models to assess the impact of parameter uncertainty on model predictions (Nossent et al., 2011). In our study, we adopted Saltelli's modified Sobol method (Please refer to Appendix A) to accurately calculate the first-order, second-order, and total-order sensitivity indices, providing a detailed understanding of the influence of each parameter on the model output. The SALib library by Herman and Usher (2017) in Python was used to determine the sensitivity of PARR to different aquifers and well parameters with Sobol's indices. In this section, we have determined the sensitivity of PARR to the four aquifer parameters (1. Hydraulic conductivity (H_k), 2. Storage coefficient (S_s or S_y), 3. Vertical anisotropy ($VANI$), and 4. Horizontal anisotropy ($HANI$)) and two well parameters (1. Well screen size (L_{sc}) and 2. Well screen location (H_{sc})). The three Sobol indices viz 1st order (S1), 2nd order (S2) and total index (ST) have been computed and presented in **Figure 7.6**. The 2nd-order Sobol's index represents the interaction between two parameters and has been represented in **Figure 7.6** (1B and 2B).

For the confined aquifer, all parameters (H_k , S_y , $VANI$, $HANI$, L_{sc} , H_{sc}) have high first-order sensitivity indices (S1), indicating that each parameter strongly affects the output variance. The sensitivity of VANI has not been apparent during the local sensitivity analysis due to the fully penetrating well. The S1 highlights the effect of partial penetrating well on the sensitivity of PARR to VANI. The total sensitivity indices (ST) are higher than the first-order indices, suggesting high parameter interactions. The interaction effect between pairs of parameters by S2 indicates that all the parameters' pairs significantly affect the sensitivity. The interaction between $VANI$ and H_{sc} is the most

significant, indicating a strong dependency between these two parameters **Figure 7.6** (1B). Apart from this, H_{sc} shows significantly high parameter interaction with all the parameters, showing the importance of partial penetrating well on the aquifer capacity.

In the case of an unconfined aquifer (**Figure 7.6(2A)**), all the parameters have high total sensitivity except $HANI$, although it still contributes through interaction. The first-order index is relatively lower compared to confined aquifers. The $VANI$ and L_{sc} have the lowest $S1$ values, which implies that the direct influence of these parameters on the PARR is less, and the sensitivity relies on the interactions. The H_k , S_y , and H_{sc} have higher direct and total contributions.

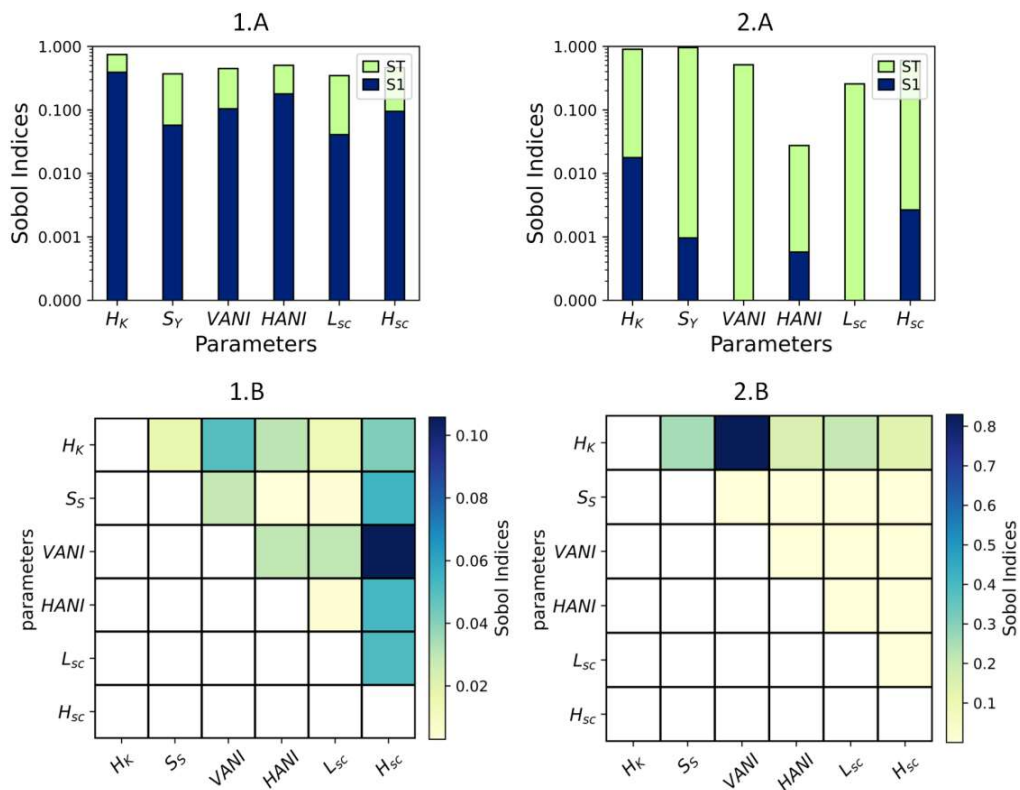


Figure 7.6.1A-1B. Sobol Indices $S1$, ST , and $S2$ for PARR in the confined aquifer; **2A-2B.** Sobol Indices $S1$, ST , and $S2$ for PARR in unconfined aquifer

The parameter H_k interacts significantly with $VANI$ in both aquifer types, indicating that hydraulic conductivity and vertical anisotropy are closely linked in their influence on PARR. The unconfined aquifer shows higher interaction effects for the pair H_k and $VANI$ than the confined aquifer. In the confined aquifer, H_k interacts more broadly with multiple parameters ($VANI$, $HANI$, L_{sc}), suggesting that the influence of hydraulic conductivity is distributed among several parameters. In the unconfined aquifer, the interactions are more concentrated, with the most substantial interaction being between H_k and $VANI$. The confined aquifer exhibits stronger second-order interactions between specific parameter pairs, indicating that parameter combinations have a more pronounced effect on the PARR, potentially due to the confined nature restricting flow and increasing dependency on specific parameters (Shandilya et al., 2022a; Sun et al., 2018). The phenomenon is justified by the response of the aquifer to pumping, where the pressure drop leads to drawdown, affecting how quickly water can be replenished from surrounding areas, which essentially depends upon the hydraulic parameter combination (Chahar, 2015; Houben, 2015). The interplay between the pressure head and the aquifer's hydraulic properties (Pyne, 2017) means that parameter combinations have amplified effects on PARR due to these dynamic responses.

7.5 DISCUSSION

7.5.1 PARR and recoverable head

The PARR for the base conditions (Table 7.1) with a varying injection duration (*from seconds to Months*) has been determined using the presented methodology. The permissible head for the given conceptual model in the case of an unconfined aquifer is taken as 57m (*3 meters below ground level (mbgl)*) and 90 m for a confined aquifer (*arbitrarily taken to represent a hypothetical overburden layer*). The recoverable head for

the hypothetical unconfined aquifer was 4.44m ($H_{per} = 57\text{m}$ and $h_0 = 52.56\text{ m}$), and for the hypothetical confined layer, it was 32.44m ($H_{per} = 90\text{m}$ and $h_0 = 57.56\text{ m}$). The PARR has been presented with respect to unit recoverable heads to make the results comparable between confined and unconfined aquifers.

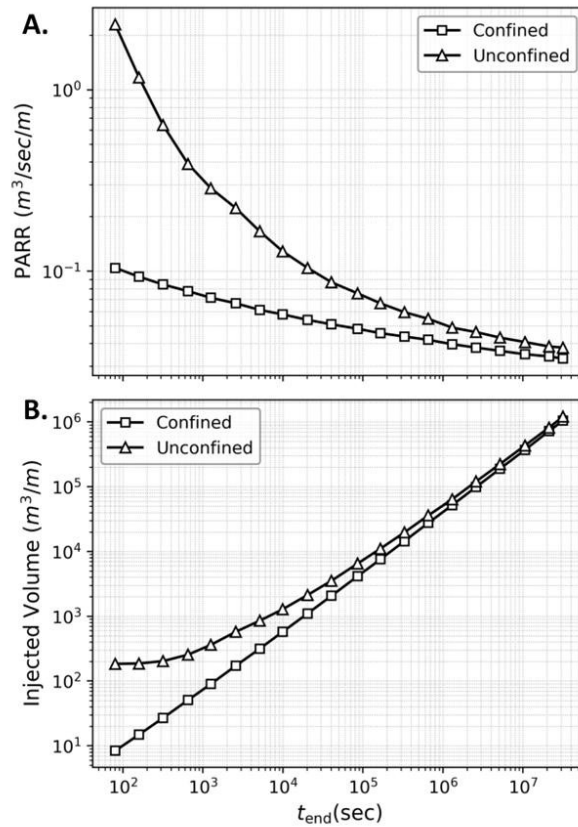


Figure 7.7. (a) variation of PARR per unit recoverable head w.r.t injection duration and (b) The injected volume per unit recoverable head corresponding to the PARR.

The PARR values are initially high for short injection durations and decrease over time (**Figure 7.7A**). This trend reflects the decrease in the injection rate required to reach the permissible head as the duration increases. In the unconfined aquifer, the decline in PARR with respect to the t_{end} is initially steep, which further attenuates.

For shorter injection durations, the unconfined aquifer exhibits significantly higher PARR values—approximately 14 times greater than those observed in the confined case. However, as the injection duration increases, the difference between the two cases diminishes, following a general power-law relationship. This behaviour is attributed to the distinct hydrodynamic responses of confined and unconfined systems. In unconfined aquifers, delayed gravity drainage affects the rate of head decline (Freeze and Cherry, 1979). The initial condition of the water table and the effects of gravity drainage led to a rapid initial rise in the head, which is then moderated over time (Huang et al., 2019), resulting in a steep decline in the PARR for short durations.

The maximum volume injected within the constraint of permissible head and duration is called the aquifer's injection capacity (Shandilya et al., 2022a). The injection capacity was calculated by multiplying the PARR with the injection duration, presented in Error! Reference source not found. **(b)**. For the confined aquifer, the injection capacity per unit recoverable head increases sub-linearly with respect to the injection duration, indicating a steady accumulation of injected volume. In contrast, the unconfined aquifer initially exhibits a slower rate of increase, reflecting the delayed propagation of pressure and groundwater head buildup. This is likely due to the gradual rise of the water table, which influences the effective storage characteristics of the system (Welch et al., 2013).

The injection capacity in the unconfined aquifer accelerates with t_{end} , reducing the difference between the two cases. For longer injection durations ($t_{end} > 10^5$ sec), the injection capacity curves for both aquifers become nearly parallel, indicating that the influence of initial transient effects in the unconfined case diminishes. This suggests that, at large time scales, the storage behaviour of confined and unconfined aquifers becomes more comparable.

7.5.2 PARR in VRB

The PARR for VRB has been determined with the calibrated GW model (chapter 5). The methodology to determine PARR for the numerical model discussed above has been used to determine PARR at each model grid location and for two layers (layer-1 and layer-3). Layer 1 comprises the shallow aquifers, which contain all the SW features, while layer 3 contains all the pumping wells in the study area. Deeper aquifer layers are currently not used and have been neglected, as analysis for these layers is sufficient for the thesis objective of river baseflow restoration. Since the PARR depends on the injection duration, the PARR for three durations (15 days, 1 month, and monsoon season (3 months on excess runoff)) have been determined and plotted below (Figure 7.8 and Figure 7.9).

The PARR values are following the aquifer heterogeneity and its spatial variability. Since the aquifers in VRB have been modeled as leaky aquifer systems (i.e., layer 2 is an aquitard and can conduct water from upper and lower aquifers), the PARR does not show very large variation across layers. The PARR has been plotted per unit of recoverable heads to have a comparable result. The PARR decreases with injection duration, as discussed in the previous section. The higher values of PARR have been observed in the zones of large hydraulic conductivities at the middle part of upper VRB in between the Varuna and Basuhi Rivers. The area after the confluence of the Varuna and Basuhi and in the lower part of the basin has also been shown as a hotspot of high recharge capacity. The large PARR values in this area represent suitable sites to plan any MAR project if an adequate water source is available.

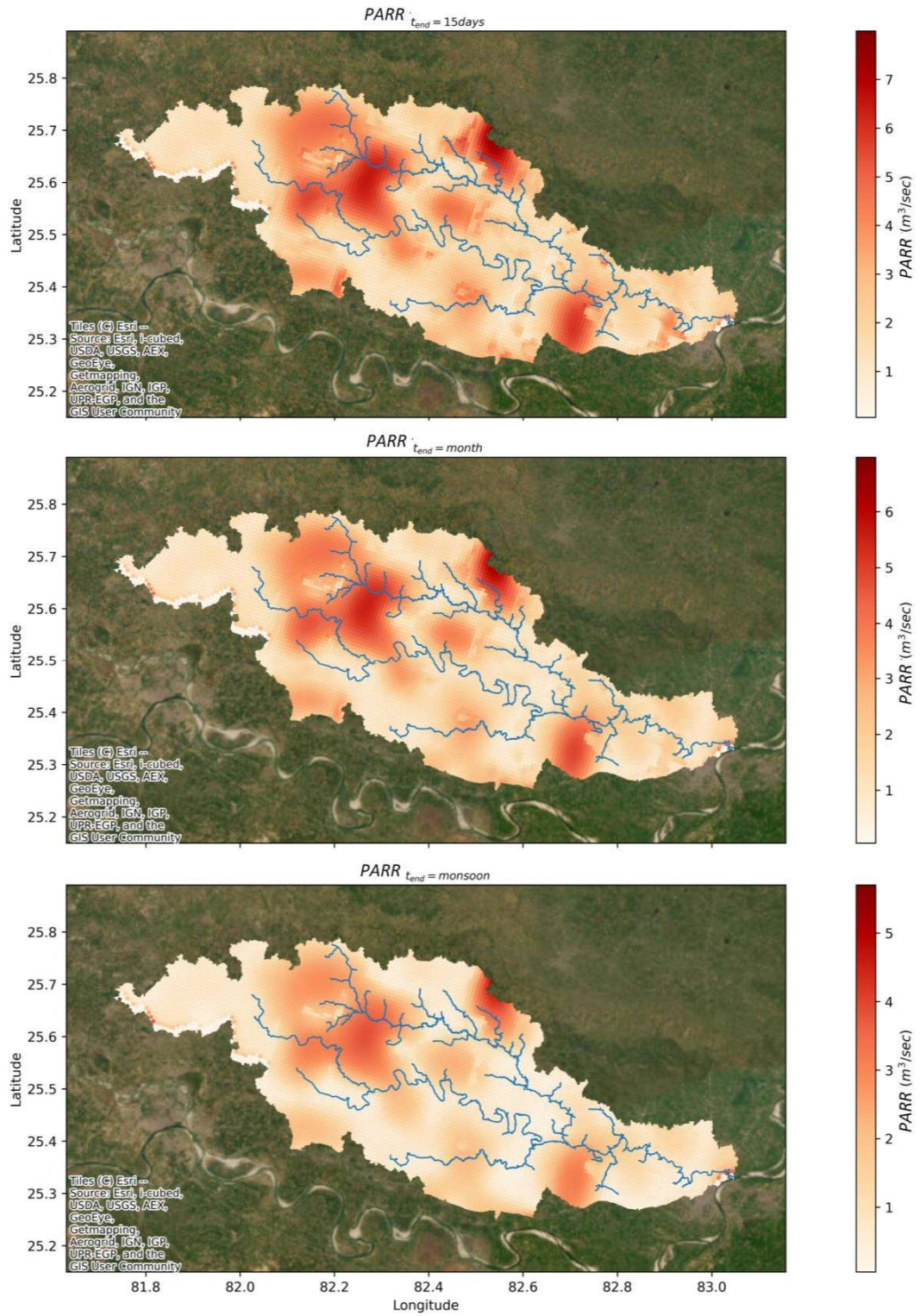


Figure 7.8. PARR values in VRB for Layer 1 (Shallow aquifer)

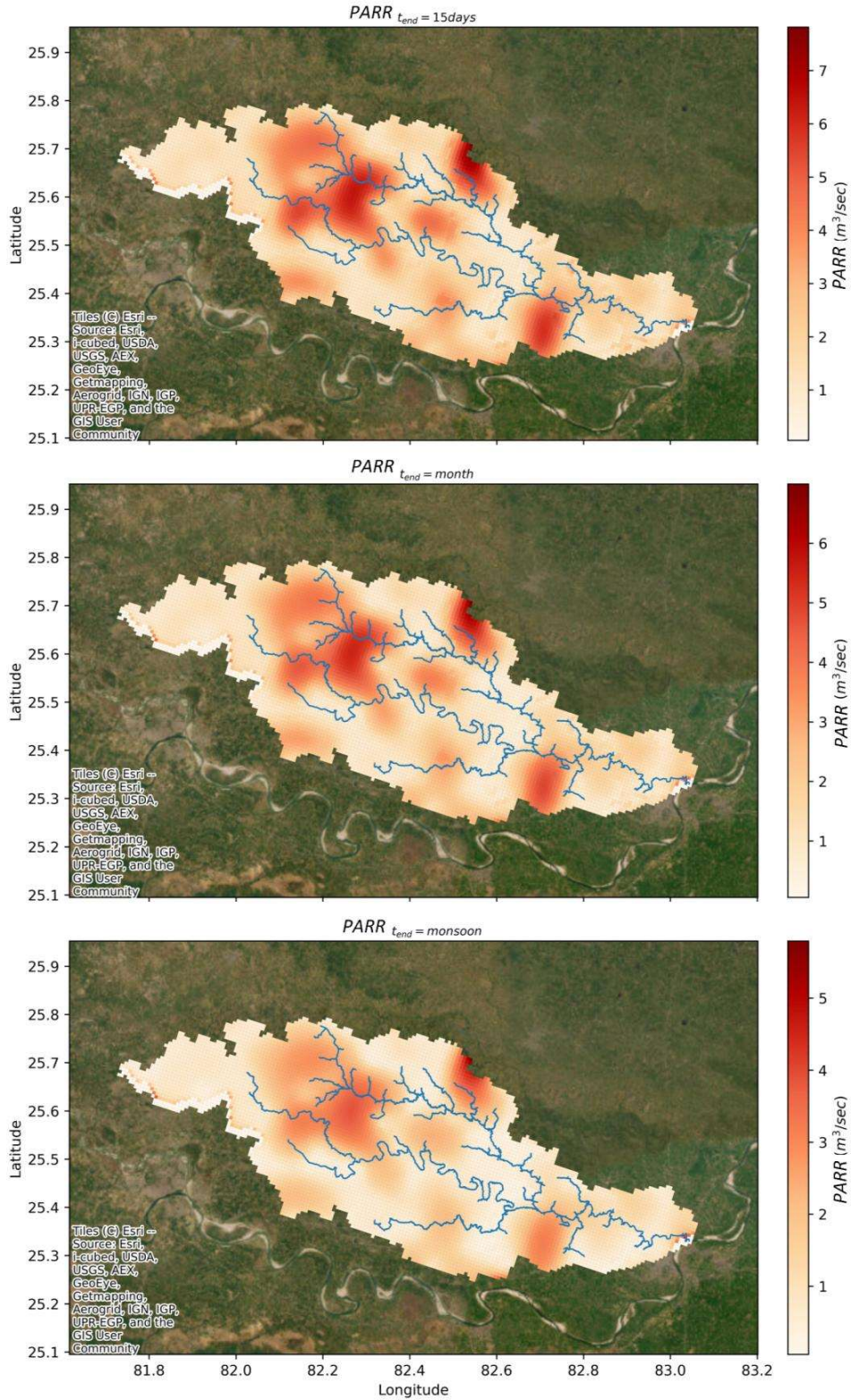


Figure 7.9. PARR values for layer 3 (Deep aquifer)

7.6 SUMMARY

This research introduces a novel optimization approach to determine the Permissible Aquifer Recharge Rate (PARR) through the use of numerical GW flow models. The study presents a detailed conceptualization of PARR, explores the various factors that affect it, and includes results from local and global sensitivity analyses based on Sobol's indices.

Key findings indicate that this new method for calculating PARR, which utilizes an adaptive learning rate based on the analytical solution for wells, is more efficient than traditional gradient descent methods, requiring fewer iterations. The research also reveals that the location and size of the well screen significantly impact PARR, with optimal placement near the bottom of the aquifer yielding higher recharge capacities.

Additionally, the sensitivity analysis highlights that PARR is particularly affected by specific interactions among parameters, notably hydraulic conductivity and vertical anisotropy in unconfined aquifers. This underscores the importance of carefully managing unconfined aquifers, taking into account the interplay of these critical factors. For confined aquifers, the results indicate a more distributed sensitivity across multiple parameters, suggesting a broader influence on PARR.

Finally, the study's application in the Varuna River Basin demonstrates the spatial variability of PARR driven by aquifer characteristics. The area downstream from the confluence of the Varuna and Basuhi rivers has been identified as a hotspot for high recharge capacity, making it a promising site for Managed Aquifer Recharge (MAR) projects, assuming a suitable water source is available.
